做科研，非一朝一夕

买器材，应速战速决

Newport数千种优质产品当日发货，
更多惊喜尽在PhotonSpeed™光速购！

mks | Newport™

CHINESE OPTICS LETTERS

Vol. 19, No. 5 | May 2021

Structural-colored silk based on Ti–Si bilayer

Jiao Chu (楚 娇)[1], Jiajun Wang (王佳俊)[1], Jie Wang (王 杰)[1], Xiaohan Liu (刘晓晗)[1,3], Yafeng Zhang (张亚峰)[2*], Lei Shi (石 磊)[1,3**], and Jian Zi (资 剑)[1,3***]

[1] State Key Laboratory of Surface Physics, Key Laboratory of Micro- and Nano-Photonic Structures (Ministry of Education) and Department of Physics, Fudan University, Shanghai 200433, China

[2] State Key Laboratory of Infrared Physics, Shanghai Institute of Technical Physics, Chinese Academy of Sciences, Shanghai 200083, China

[3] Collaborative Innovation Center of Advanced Microstructures, Fudan University, Shanghai 200433, China

*Corresponding author: zhangyf@mail.sitp.ac.cn

**Corresponding author: lshi@fudan.edu.cn

***Corresponding author: jzi@fudan.edu.cn

Received July 26, 2020 | Accepted November 26, 2020

In this Letter, Ti–Si bilayer was deposited on white silk to achieve coloration of the silk. By controlling the thickness of the Ti layer and Si layer, the saturation and the hue of the color on the silk could be preciously modulated, respectively. The structural colors on the silk could cover the major colors in the International Commission on Illumination 1931 chromaticity diagram, and it exhibits good durability, which is demonstrated by rubbing and stretching treatments. The developed textile coloration method may provide an eco-friendly technology in the silk dyeing industry.

Keywords: structural color; silk coloration; Ti-Si bilayer.

DOI: 10.3788/COL202119.051601

1. Introduction

Textile dyeing plays an indispensable role in our daily life, enriching people's choices of the textile and satisfying our desire for aesthetics. In general, traditional textile dyeing is mainly based on chemical pigments, which may lead to environmental pollution and health concerns[1,2]. Fortunately, structural colors found in the natural world inspire people to utilize nanostructures to achieve coloration that could avoid the above-mentioned problems. Structural colors[3–11] originate from the interaction of light with photonic structures whose feature sizes are comparable to visible wavelengths[12,13]. There are many kinds of structural colors in the bio-world including the structural-color patterns in the transparent wings of small Hymenoptera[14], the brilliant metallic green color based on multilayers in the jeweled beetle[15], the colorful eye patterns composed of two-dimensional (2D) photonic crystals in the peacock[16], and so on[17–20]. Inspired by these natural structures, we can also fabricate some similar structures with eco-friendly and non-toxic materials to replace dye. Over the last few decades, a series of explorations focusing on the bio-inspired fabrication of structural colors have been implemented: seashell-inspired 2D photonics nanostructures could be employed for solar energy conversion applications[21]; chameleon-inspired photonic film could be employed for visual senses[22]; bird-feather-inspired amorphous structures could be employed for structural color ink[23]. In this work, structural color based on the thin-film interference[24,25] effect was applied to white silk fabrics. Ti was chosen as the adsorbed and adhesion layers, and we could adjust the saturation of the color by controlling the thickness of the Ti layer. The Si layer was deposited on the Ti layer, and the hue could be regulated by changing the thickness of the Si layer. Compared with traditional textile dyeing, our method could be non-toxic and eco-friendly, and the color could be tuned precisely.

In order to construct color coatings on silk, we deposited Ti–Si bilayers on white silk using e-beam evaporation. Silk, composed of protein, is an eco-friendly biological material[26,27] with many remarkable properties such as breathability, hygroscopicity[28,29], and elegant shine[30]. Besides, it is abundantly available on the earth, so silk has been popular in people's daily life for thousands of years. Natural silk is white and usually dyed by chemical pigments in the past to bring out the individual and cultural identities. In our work, we select white silk as the substrate, and the coloration is established on a nanostructure of the Ti–Si bilayer. Our structural color system consists of Ti and Si. Ti is beneficial to increase the adhesion between silk fabrics and the Si layer. What is more, Ti could also play the role of an absorption layer because of its high absorption rate in the visible frequency, which is important to improve the color saturation. The Si layer is mainly used to modulate the color. The large refractive index of Si guarantees the capability of our structure to obtain an obvious variation in hue by slightly changing the

thickness of the Si layer, and it is essential for cost-effective fabrication[31–33].

2. Results and Discussions

Figure 1(a) shows the illustration of structural-colored silk. The white line represents the white silk, while the gray line adjacent to the white line represents silk coated with a Ti layer, and the dark red line represents silk coated with a Ti–Si bilayer structure. Figure 1(b) shows the scanning electron microscope image of the Ti–Si bilayer on a single fiber. The sample reveals well-defined layers. The black part in the upper right area is the silk. The central area with the cyan mask is the Ti layer, and the area with purple mask is the Si layer. Figure 1(c) shows the photograph of three typical macro samples by introducing the Ti–Si bilayer on white silk. We obtain cyan, olive, and brick red structural-colored silk with the Si layer equal to 54 nm, 87 nm, and 120 nm, respectively, and the Ti layer is fixed at 100 nm. Both the single Si layer and single Ti layer coated on the white silk could not get a pretty color, as shown in Figs. 1(d) and 1(e).

Figure 2(a) shows the photograph of structural-colored silk by changing the thickness of the Ti layer and the thickness of the Si layer. Vertically, saturation enhancement occurs when increasing the thickness of the Ti layer. Horizontally, the hues range from indigo to purple red by increasing the thickness of the Si layer. Figure 2(b) shows the measured reflectance spectra of samples in Fig. 2(a) with the thickness of the Si layer varied from 54 nm to 120 nm, and the thickness of the Ti layer fixed at 100 nm, revealing a distinct redshift. Figure 2(c) shows the measured reflectance spectra of the samples in the third column of Fig. 2(a) with the thickness of the Si layer fixed at 54 nm. With the thickness of the Ti layer increasing, the reflectance at the visible frequency decreases gradually, resulting in the enhancement of saturation. As shown in Fig. 2(d), the measured reflectance spectrum of ten samples in the first row of Fig. 2(a) is converted into the International Commission on Illumination (CIE) 1931 chromaticity values. The ten points cover the main colors in the chromaticity diagram, indicating that the structural-colored silk is universal in color representation. We do not observe color changes with the naked eye at oblique angles ($< 50°$), and this is due to the high refractive index of the Si layer. We measured

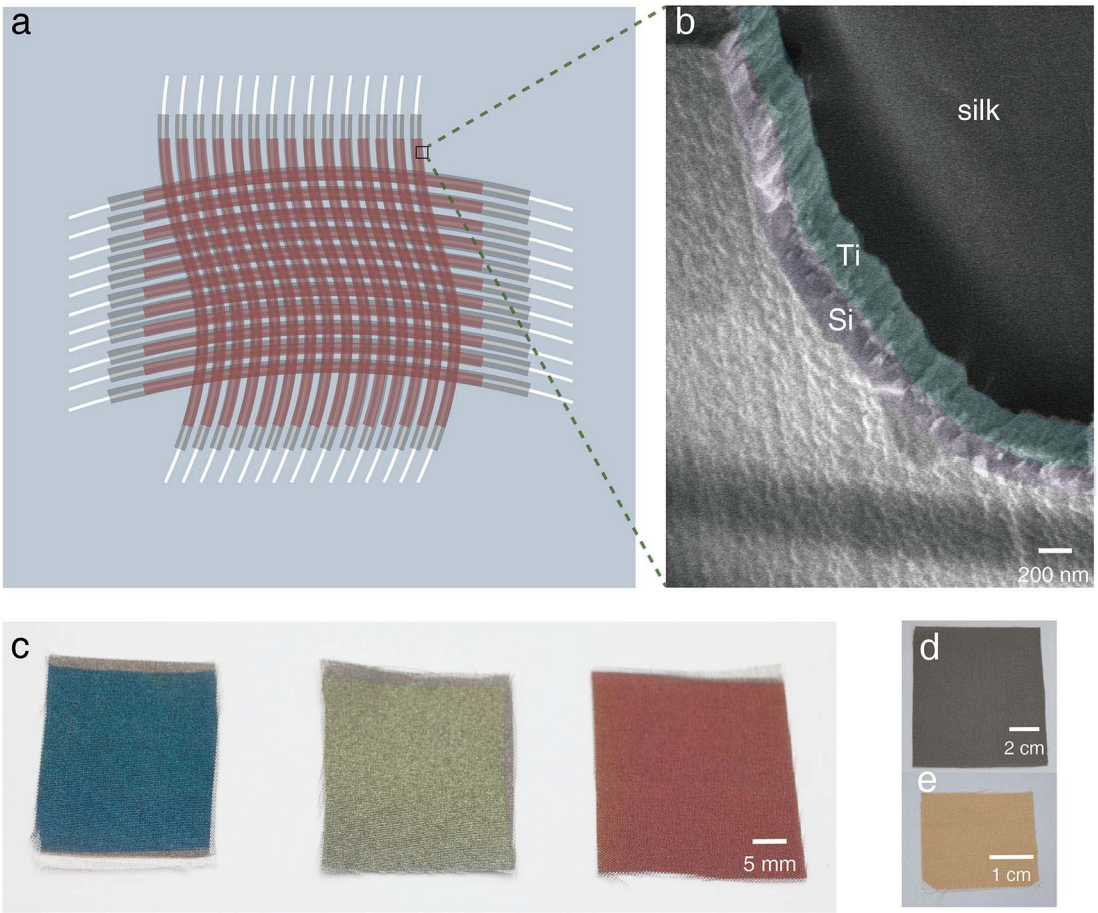

Fig. 1. (a) Illustration of the proposed bilayer for realization of structural color on white silk. The white line represents silk, while the gray line represents silk coated by a Ti layer, and the dark red line represents silk coated with a Ti–Si bilayer structure. (b) SEM image of the Ti–Si bilayer on a single fiber. The Ti layer is marked by cyan, and the Si layer is marked by purple. (c) Photograph of cyan, olive, and brick red coatings on white silk. The thickness of the Si layer is 54 nm, 87 nm, and 120 nm with the Ti layer fixed at 100 nm. (d) Photograph of silk fabric with a Ti layer thickness of 100 nm. (e) Photograph of 105 nm Si layer on white silk.

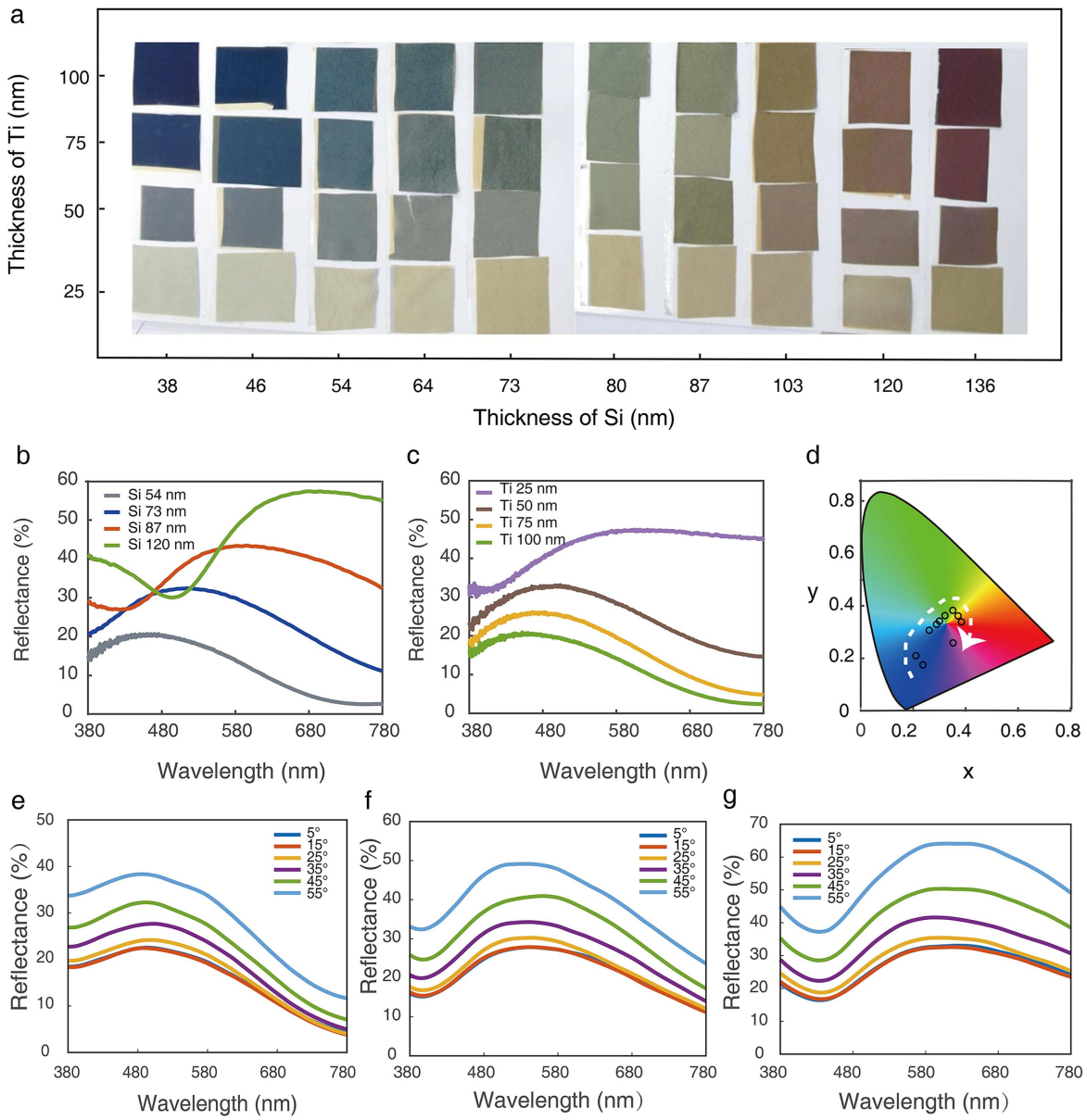

Fig. 2. (a) Color palette of the structural colors as a function of the thicknesses of the Ti layer and Si layer. (b) Measured reflectance spectra of four bilayers with the Si layer thickness varied from 54 nm to 120 nm. The thickness of the Ti layer is fixed at 100 nm. For comparison, the blue, orange, and green spectra are offset up by 5%, 10%, and 15%, respectively. (c) Measured reflectance spectra of four bilayers with the Ti layer thickness varied from 25 nm to 100 nm. The thickness of the Si layer is fixed at 54 nm. (d) Corresponding colors of samples in the first row of (a) in the CIE 1931 chromaticity diagram. The thickness of the Si layer increases along the direction of the arrow. (e)–(g) Measured angle-resolved specular reflectance spectra of three samples. The thickness of the Si layer in (e), (f), and (g) is 64 nm, 80 nm, and 87 nm, respectively. The thickness of the Ti layer is fixed at 100 nm.

the refractive index of the deposited Si layer by using an ellipsometer, showing that the refractive index of Si is relatively high, around 3.46 at 580 nm. As shown in Figs. 2(e)–2(g), when changing the incident angle from 5 to 55 deg, the wavelength of the reflection peak almost does not shift. This indicates that the colors modulated by the Ti–Si bilayer on the white silk are nearly angle-independent in the measured angle range.

Figure 3 shows two photographs of Beijing Opera Facial Makeup on white silk. We can observe the vivid facial features of the Beijing Opera Facial Makeup by changing the thicknesses

Fig. 3. Structural-colored Beijing Opera Facial Makeup patterns on white silk.

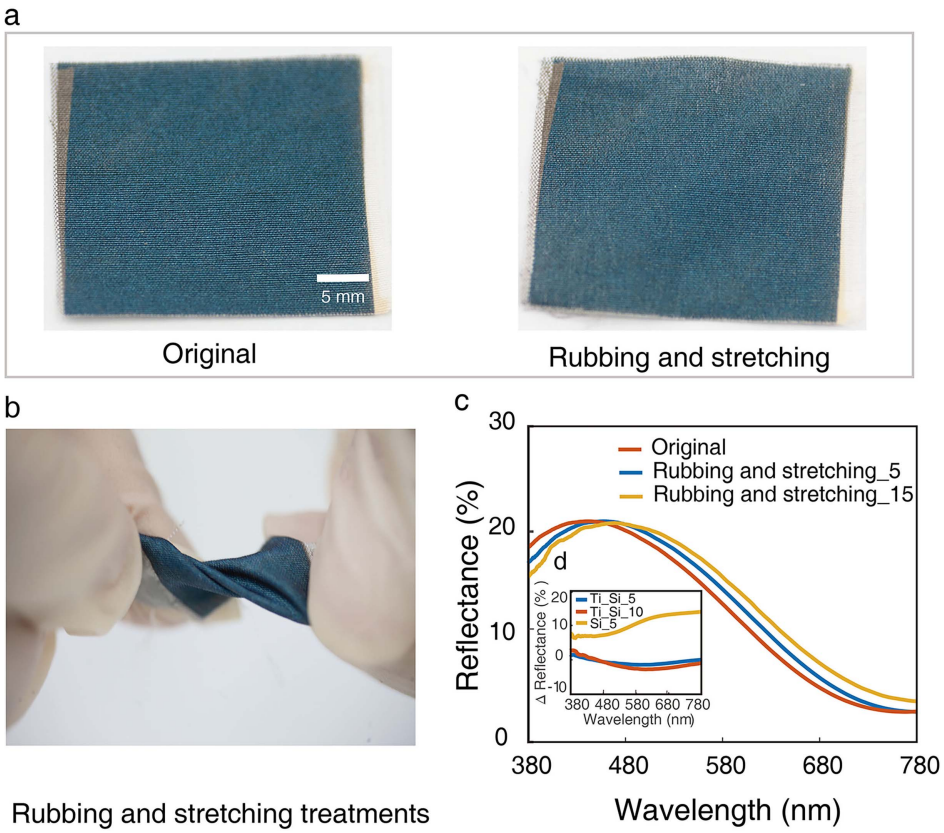

Fig. 4. (a) Photograph of cyan coatings on white silk before (original) and after rubbing and stretching treatments. (b) Photograph of cyan coatings on white silk with rubbing and stretching treatments. (c) Corresponding reflectance spectra for the cyan coatings on white silk before (original) and after rubbing and stretching treatments for 5 and 15 times. (d) Changes of the reflectance after rubbing and stretching treatments (Δ reflectance) for the Ti–Si bilayer and single Si layer.

of the Ti layer and the Si layer. In order to avoid the shadow of the camera, the photograph is taken at about 20°. In fact, there is nearly no difference between the color of the photograph and the color actually seen at the normal angle, revealing a similar coloring effect to traditional dyeing.

Figure 4(a) shows the photograph of cyan-colored silk before and after rubbing and stretching treatments. The rubbing and stretching treatments are shown in Fig. 4(b). Figure 4(c) shows the corresponding reflectance spectra. Although there is a small change at the peak position before and after rubbing treatments for 5 or 15 times, color fading is not observed in Fig. 4(a). For the sample with only a 105 nm Si layer, there is a decrease of more than 10% of the reflectance after rubbing and stretching treatments, as shown in Fig. 4(d). While for the sample with the Ti–Si bilayer (rubbing and stretching treatments for 5 or 15 times), the change of reflectance is about 2%, indicating that the Ti layer can act as an adhesion layer. The structural-colored silk exhibits good durability, demonstrating potential practical applications of the structural-colored silk.

3. Conclusion

In summary, we propose and demonstrate a non-toxic, eco-friendly, and cost-effective structural-colored silk based on the thin-film interference effect by constructing a Ti–Si bilayer on white silk. Enabled by the absorption of Ti in the visible frequency, we can obtain high-saturation colors on the silk. By changing the thickness of the Si layer, we can achieve the major colors in the CIE 1931 chromaticity diagram. Meanwhile, the structural color is insensitive to the change of observation angle ($< 50°$). In addition, rubbing and stretching treatments show that these vivid structural colors coated on silk possess good durability, indicating a potential method for developing green technologies in the silk dyeing industry.

Acknowledgement

The work was supported by the China National Key Basic Research Program (Nos. 2016YFA0301103, 2016YFA0302000, and 2018YFA0306201) and the National Natural Science Foundation of China (Nos. 11774063, 11727811, 91750102, and 91963212). L. Shi was further supported by the Science and Technology Commission of Shanghai Municipality (Nos. 19XD1434600, 2019SHZDZX01, and 19DZ2253000).

References

1. A. Khatri, M. H. Peerzada, M. Mohsin, and M. White, "A review on developments in dyeing cotton fabrics with reactive dyes for reducing effluent pollution," J. Clean. Prod. **87**, 50 (2015).

2. D. Philips, "Environmentally friendly, productive and reliable: priorities for cotton dyes and dyeing processes," J. Soc. Dye. Colour. **112**, 183 (1996).
3. Z. Yang, Y. Zhou, Y. Chen, Y. Wang, P. Dai, Z. Zhang, and H. Duan, "Reflective color filters and monolithic color printing based on asymmetric Fabry–Perot cavities using nickel as a broadband absorber," Adv. Opt. Mater. **4**, 1196 (2016).
4. Y. Chen, X. Duan, M. Matuschek, Y. Zhou, F. Neubrech, H. Duan, and N. Liu, "Dynamic color displays using stepwise cavity resonators," Nano Lett. **17**, 5555 (2017).
5. Y. Gao, C. Huang, C. Hao, S. Sun, L. Zhang, C. Zhang, Z. Duan, K. Wang, Z. Jin, N. Zhang, A. V. Kildishev, C.-W. Qiu, Q. Song, and S. Xiao, "Lead halide perovskite nanostructures for dynamic color display," ACS Nano **12**, 8847 (2018).
6. P. Mao, C. Liu, F. Song, M. Han, S. A. Maier, and S. Zhang, "Manipulating disordered plasmonic systems by external cavity with transition from broadband absorption to reconfigurable reflection," Nat. Commun. **11**, 1538 (2020).
7. F. Chen, H. Yang, K. Li, B. Deng, Q. Li, X. Liu, B. Dong, X. Xiao, D. Wang, Y. Qin, S.-M. Wang, K.-Q. Zhang, and W. Xu, "Facile and effective coloration of dye-inert carbon fiber fabrics with tunable colors and excellent laundering durability," Acs Nano **11**, 10330 (2017).
8. Q. Fu, H. Zhu, and J. Ge, "Electrically tunable liquid photonic crystals with large dielectric contrast and highly saturated structural colors," Adv. Funct. Mater. **28**, 1804628 (2018).
9. D. Yang, Y. Qin, S. Ye, and J. Ge, "Polymerization-induced colloidal assembly and photonic crystal multilayer for coding and decoding," Adv. Funct. Mater. **24**, 817 (2014).
10. C. Liu, Y. Long, B. Yang, G. Yang, C.-H. Tung, and K. Song, "Facile fabrication of micro-grooves based photonic crystals towards anisotropic angle-independent structural colors and polarized multiple reflections," Sci. Bull. **62**, 938 (2017).
11. X. Zhu, M. K. Hedayati, S. Raza, U. Levy, N. A. Mortensen, and A. Kristensen, "Digital resonant laser printing: bridging nanophotonic science and consumer products," Nano Today **19**, 7 (2018).
12. J. Zi, B. Dong, T. Zhan, and X. Liu, "Photonic structures for coloration in the biological world," in *Bioinspiration* (Springer, 2012), p. 275.
13. J. Sheng, J. Xie, and J. Liu, "Multiple super-resolution imaging in the second band of gradient lattice spacing photonic crystal flat lens," Chin. Opt. Lett. **18**, 120501 (2020).
14. E. Shevtsova, C. Hansson, D. H. Janzen, and J. Kjærandsen, "Stable structural color patterns displayed on transparent insect wings," Proc. Natl. Acad. Sci. **108**, 668 (2011).
15. V. Sharma, M. Crne, J. O. Park, and M. Srinivasarao, "Structural origin of circularly polarized iridescence in jeweled beetles," Science **325**, 449 (2009).
16. J. Zi, X. Yu, Y. Li, X. Hu, C. Xu, X. Wang, X. Liu, and R. Fu, "Coloration strategies in peacock feathers," Proc. Natl. Acad. Sci. **100**, 12576 (2003).
17. S. Berthier, *Iridescences: The Physical Colors of Insects* (Springer Science & Business Media, 2007).
18. S. Kinoshita, S. Yoshioka, and J. Miyazaki, "Physics of structural colors," Rep. Prog. Phys. **71**, 076401 (2008).
19. J. P. Vigneron and P. Simonis, "Natural photonic crystals," Phys. B Condens. Matter **407**, 4032 (2012).
20. A. R. Parker, V. L. Welch, D. Driver, and N. Martini, "Opal analogue discovered in a weevil," Nature **426**, 786 (2003).
21. Z. Sun, T. Liao, W. Li, Y. Qiao, and K. Ostrikov, "Beyond seashells: bioinspired 2D photonic and photoelectronic devices," Adv. Funct. Mater. **29**, 1901460 (2019).
22. G. H. Lee, T. M. Choi, B. Kim, S. H. Han, J. M. Lee, and S.-H. Kim, "Chameleon-inspired mechanochromic photonic films composed of non-close-packed colloidal arrays," ACS Nano **11**, 11350 (2017).
23. M. Xiao, Z. Hu, Z. Wang, Y. Li, A. D. Tormo, N. Le Thomas, B. Wang, N. C. Gianneschi, M. D. Shawkey, and A. Dhinojwala, "Bioinspired bright noniridescent photonic melanin supraballs," Sci. Adv. **3**, e1701151 (2017).
24. K. Cao, L. Chen, K. Cheng, Z. Sun, and T. Jia, "Regular uniform large-area subwavelength nanogratings fabricated by the interference of two femtosecond laser beams via cylindrical lens," Chin. Opt. Lett. **18**, 093201 (2020).
25. H. Yang, F. Zhang, L. Leng, Z. Zeng, Y. Shao, H. Zhang, N. Yang, and X. Chen, "Grating coupler efficiency enhancement by double layer interference," Chin. Opt. Lett. **17**, 030501 (2019).
26. Y. Yang, H. Wang, F.-Y. Yan, Y. Qi, Y.-K. Lai, D.-M. Zeng, G. Chen, and K.-Q. Zhang, "Bioinspired porous octacalcium phosphate/silk fibroin composite coating materials prepared by electrochemical deposition," ACS Appl. Mater. Interfaces **7**, 5634 (2015).
27. Y. Wang, M. Li, and Y. Wang, "Silk: a versatile biomaterial for advanced optics and photonics," Chin. Opt. Lett. **18**, 080004 (2020).
28. M. Khatri, N. Hussain, S. El-Ghazali, T. Yamamoto, S. Kobayashi, Z. Khatri, F. Ahmed, and I. S. Kim, "Ultrasonic-assisted dyeing of silk fibroin nanofibers: an energy-efficient coloration at room temperature," Appl. Nanosci. **10**, 917 (2020).
29. Q. Wang, C. Wang, M. Zhang, M. Jian, and Y. Zhang, "Feeding single-walled carbon nanotubes or graphene to silkworms for reinforced silk fibers," Nano Lett. **16**, 6695 (2016).
30. Q. Li, Y. Zhang, L. Shi, H. Qiu, S. Zhang, N. Qi, J. Hu, W. Yuan, X. Zhang, and K.-Q. Zhang, "Additive mixing and conformal coating of noniridescent structural colors with robust mechanical properties fabricated by atomization deposition," ACS Nano **12**, 3095 (2018).
31. W. Yang, S. Xiao, Q. Song, Y. Liu, Y. Wu, S. Wang, J. Yu, J. Han, and D.-P. Tsai, "All-dielectric metasurface for high-performance structural color," Nat. Commun. **11**, 1864 (2020).
32. Z. Dong, J. Ho, Y. F. Yu, Y. H. Fu, R. Paniagua-Dominguez, S. Wang, A. I. Kuznetsov, and J. K. W. Yang, "Printing beyond sRGB color gamut by mimicking silicon nanostructures in free-space," Nano Lett. **17**, 7620 (2017).
33. X. Zhu, W. Yan, U. Levy, N. A. Mortensen, and A. Kristensen, "Resonant laser printing of structural colors on high-index dielectric metasurfaces," Sci. Adv. **3**, e1602487 (2017).